Design and construction of a guarded hot plate apparatus operating down to liquid nitrogen temperature

Manfeng Li,[1,2] Hua Zhang,[1] and Yonglin Ju[1,a)]
[1]*Institute of Refrigeration and Cryogenics, Shanghai Jiao Tong University, Shanghai 200240, People's Republic of China*
[2]*Institute of Environmental and Municipal Engineering, North China University of Water Resources and Electric Power, Zhengzhou 450011, People's Republic of China*

(Received 11 January 2012; accepted 17 June 2012; published online 10 July 2012)

A double-sided guarded hot plate apparatus (GHP) is specifically designed, fabricated, and constructed for the measurement of thermal conductivities of insulation specimens operated down to liquid nitrogen temperature (−196 °C), at different controlled pressures from 0.005 Pa to 0.105 MPa. The specimens placed in this apparatus are 300 mm in diameter at various thicknesses ranging from 4 mm to 40 mm. The apparatus is different from traditional GHP in terms of structure, supporting and heating method. The details of the design and construction of the hot plate, the cold plates, the suspensions, the clampings, and the vacuum chamber of the system are presented. The measurement methods of the temperatures, the input power, the meter area, and the thickness of the specimens are given. The apparatus is calibrated with teflon plates as sample and the maximum deviation from the published data is about 6% for thermal conductivity. The uncertainties for the measurement are also discussed in this paper. © *2012 American Institute of Physics*. [http://dx.doi.org/10.1063/1.4732816]

I. INTRODUCTION

The guarded hot plate apparatus (GHP), generally recognized as the primary method, is widely used to measure thermal conductivities of homogeneous thermal insulations.[1] The apparatus is applicable to the measurement for a wide variety of specimens, from flat-slab to porous, and a wide range of environmental conditions at different temperatures and pressures.[2]

The accurate determination of thermal conductivities is critical in research, development, production, and application of thermal insulations. In particular, the thermal conductivity of thermal insulations is directly related to long-distance transport and storage of cryogenic liquids. The design and construction of the double-sided GHP are based on the applications of thermal insulations operating at liquid nitrogen temperature (−196 °C).

In recent years, a great deal of GHP has been designed and constructed for different measurement requirements of thermal conductivities. Hemminger *et al.*[3] developed a GHP for the temperature from −75 °C to 200 °C, and proposed a detailed evaluation procedure with several correction calculations for measurements on glass samples. Zarr *et al.*[4] proposed the determination of steady-state thermal transmission properties of insulations from 90 K to 900 K in a controlled gas atmosphere. The apparatus was used to measure the flat-slab specimens with 500 mm in diameter at various thicknesses ranging from 13 mm to 100 mm. Filla[5] built a one-sided very-temperature GHP to measure the thermal conductivities of monolithic ceramics, ceramic composites, thermal barrier coatings, functional graded materials, and high-temperature metal alloys from 400 K to 1400 K. The apparatus accommodated the flat-slab specimens with 70 mm in diameter and 1 mm–8 mm in thickness.

For GHP, the application of line-heat sources, the measurement methods, and the uncertainty analysis for the measurements are very important. Therefore, they have been also discussed and proposed by many researchers.

The method of line-heat sources for the meter and guard plates has been discussed by Flynn *et al.*,[6] who proposed the best position of circular heater embedded in the hot plate through theoretical analysis, calculation, and finite element simulation to obtain the uniform temperature distribution. Hahn *et al.*[7] described a line-heat sources concept, which could generate a nearly isothermal profile within a disc-shaped plate. Xaman *et al.*[8] employed a heater embedded in a central plate and guard ring to generate a heat flux, and applied the Green function formulation to compute the temperature distributions in the central plate and the guard plate. The comparison of the analytic results and the experimental measurements conducted on aluminum plates showed in good agreement with a standard deviation of 3%.

The determination and the measurement methods of input heat flow in the meter plate were proposed. Dey *et al.*[9] discussed the design and construction of the GHP for measuring the heat flow though an evacuated space between plane-parallel glass surfaces. Woodside[10] applied another solution, which was obtained by the application of two successive Schwarz transformations as well as the assumptions, which had been verified by relaxation calculation. The calculated and measured data of the error heat flow for three different hot plates showed in good agreement. Holcombe[11] proposed a new method for the GHP, which could guarantee the continuous and accurate measurement of power consumption of the test plate. The output of the temperature controller was converted into bursts of precisely regulated pulses of power, and these were counted against a time base.

a)Author to whom correspondence should be addressed. Electronic mail: yju@sjtu.edu.cn. Tel./Fax: +86 21 34206532.

The precision and bias of the test data for the GHP were also discussed. Somers *et al.*[12] analyzed the error from the convection heat loss at the exposed edges of the sample, and given the maximum errors of square and round samples in the guarded hot plate of various dimensions. Pham and Smith[13,14] proposed the analytical equations for the thermal imbalance error and given the correction to the heat flow area in GHP for isotropic and anisotropic materials. These equations had been verified and could be used to analyze the errors for circular plates and square plates when the corner effects were neglected.

In the present paper, a double-sided GHP apparatus was designed and constructed for measuring the thermal conductivities of insulation specimens operated down to liquid nitrogen temperature (−196 °C), at different controlled pressures, based on the requirements of ASTMC177-04, ASTMC1043, and ISO8302 standard test methods. The design and construction of the hot plate, the cold plates, the suspensions, the clampings, and the vacuum chamber for the system were presented in detail. The measurement methods and the uncertainties of the temperatures, the input power, the surface area, and the thickness of the specimens were also given and discussed.

II. APPARATUS

A. Theory

The basic design principle is to create a steady state, one-dimensional heat flow through the insulation materials by placing it between two isothermal plates at different temperatures with various gases and pressures.

Since the heat losses from the GHP to the surroundings are difficult to take into account, a double-sided symmetric arrangement of the GHP apparatus is adopted, as shown in Fig. 1. It consists principally of a hot plate assembly, two cold plate assemblies, a secondary guarding in the form of edge insulation, a temperature-controlled secondary edge guard, and an environmental chamber.[15] The hot plate assembly is comprised of a circular meter plate and a co-axial guard plate. The meter plate is surrounded by the guard plate with a small gap between them. In the traditional double-sided model of operation, specimens of the same material having nearly the same density, size, and thickness are placed on each surface of the hot plate and clamped by the cold plates.[16]

The meter plate is used to generate heat flux in order to maintain a desired temperature gradient across the specimen. To ensure that the heat flow generated by the meter plate through the specimens axially, the temperature difference between the meter plate and the guard plate should be kept closer enough to reduce the temperature variance of the meter plate originated from the heat gains or losses. The temperature of the meter plate can be changeable by adjusting the input power of the electrical heater that is embedded within the meter plate.[9] The surface temperatures of the two cold plate assemblies maintain below that of the hot plate by circulating liquid nitrogen.

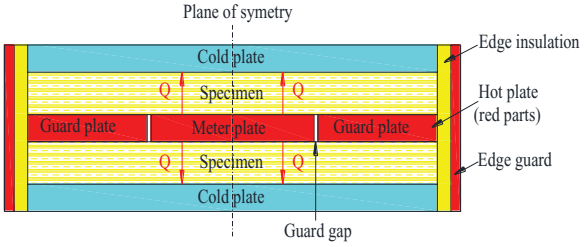

FIG. 1. The arrangement structure of the guarded hot plate apparatus.

The thermal conductivity of the specimens is calculated based on Fourier's law by the average temperature difference between the meter and cold plates, the heat input to the meter plate, the surface area of the meter plate, and the thickness of the specimens

$$Q = \lambda A \frac{\Delta T}{L}, \tag{1}$$

where λ is the thermal conductivity of the specimens, W/(m K); Q is the heat flow rate, W; A is the cross-sectional surface area of the meter plate normal to the heat flow, m^2; ΔT is the temperature difference across the specimen, °C; L is the thickness of the specimen, m.

For the double-sided mode of operation, the thermal conductivity of the specimens can be expressed as

$$\lambda = \frac{Q}{A[(\Delta T_1/L_1) + (\Delta T_2/L_2)]}. \tag{2}$$

ΔT_1 and ΔT_2 are the temperature difference across the specimens 1 and 2, °C; L_1 and L_2 are the thicknesses of the specimens 1 and 2, respectively, m.

If temperature difference across the specimens is the same, the operational definition for the mean thermal conductivity can be expressed as

$$\lambda = \frac{QL}{2A\Delta T}, \tag{3}$$

where ΔT is the temperature difference across the specimens, K; and L is the thickness of the specimens, m.

In order to minimize thermal contact resistance between the specimens and the plates, silicone oil was uniformly greased on both sides of the specimens. The layers of the silicone oil have the same thicknesses and thermal conductivities under the same clamping force, and temperature drops in the contact mediums can be reduced as

$$\Delta T_c = \lambda_c \frac{QL_c}{A}, \tag{4}$$

where ΔT_c is the temperature difference across the silicone oil, K; λ_c is the thermal conductivity of the silicone oil, W(m K); and L_c is the thickness of the silicone oil, m.

B. Apparatus description

The GHP was designed in particular for the measurement of the thermal conductivity of insulations having thicknesses of 4 mm–45 mm at liquid nitrogen temperature (−196 °C), at the controlled pressures from 0.005 Pa to 0.105 MPa.

The structure diagram of the GHP was shown in Fig. 2. It consisted primarily of a vacuum chamber, a set of suspension assemblies and a whole test component. The whole test com-

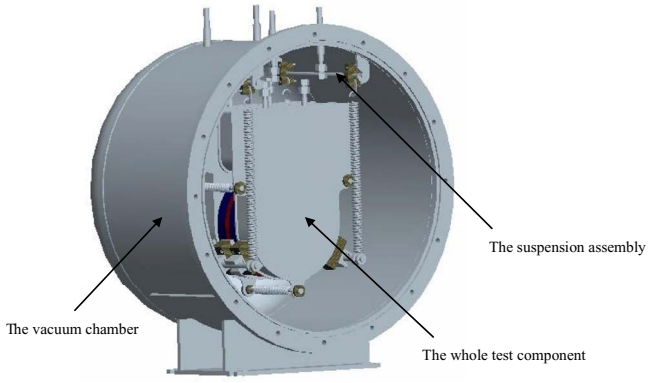

FIG. 2. Schematic design of the guarded hot plate apparatus.

ponent was typically configured in a horizontal orientation and was suspended from the suspension assemblies through the compression springs, in order to minimize the heat conducted losses. Moreover, the whole test component was enclosed by a vacuum chamber at different controlled pressures.

The detailed structure of the whole test component was illustrated in Fig. 3. The test component consisted of the hot plate assembly, the two cold plate assemblies, the sliding rods, the clamping assemblies, and the compression springs. The hot plate assembly was placed in the middle of the specimens and generated a constant heat flux through the specimens. The liquid nitrogen containers were thermally attached onto the outside surface of the specimens to keep a constant low temperature. The sliding rods were used to facilitate the installation of the test specimens, and to meet the test specimens in different thicknesses. The other function of the sliding rods was to support the hot plate assembly and the cold plate assemblies. The clamping assemblies, which was wedged into the outside panels of the liquid nitrogen containers, was employed to provide a fixed clamping force between the specimens, the hot and cold plate surfaces.

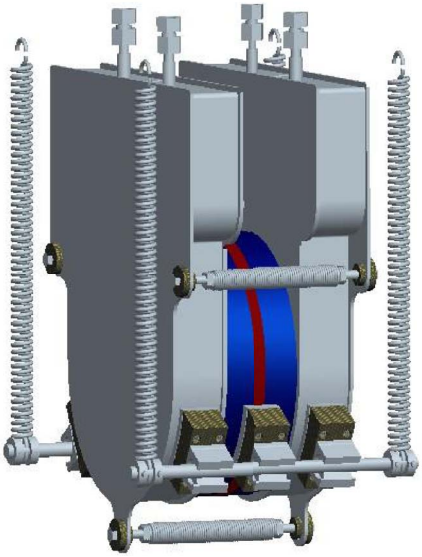

FIG. 3. Schematic design of the whole test component.

C. Specimen

The ideal specimen should be shaped like a circular cylinder of thicknesses ranging from 4 mm to 40 mm. The deviations from thicknesses, diameter, and plane parallelism of the specimen were less than ± 0.01 mm. The surfaces of the specimens should be prepared to ensure that they are parallel and have uniform thermal contact with the heating and cooling plates. Preparation and condition of the specimens should be in accordance with the appropriate material specification and condition if necessary.

A reproducible constant clamping force is imposed on the guarded-hot plate to promote good thermal contact between the hot and cold surface assemblies and the specimens and to maintain accurate spacing. The clamping force should not exceed 2.5 kPa to minimize the changes in the direction thickness and deformation of the specimens.[15]

III. CONSTRUCTION OF APPARATUS

A. Hot plate assembly

The structure of the hot plate assembly was shown in Fig. 4. The hot plate assembly generated a steady-state, one-dimensional heat flux through the specimens. It consisted of a meter plate, a guard plate, the support blocks, the sliding bearings, and a connection guard. The meter plate was comprised of a metered section heater and two metered section plates. The metered section heater was sandwiched between two metered section plates. The guard plate consisted of a guard section heater and two primary guard section plates. The guard section heater was sandwiched between two primary guard section plates.

The meter plate was placed in the center of the guard plate by three stainless steel pins, which were equally spaced around the circumference of the meter plate, and were used to adjust the uniform gap between the meter and guard plates. The support blocks and the connection guard were made of reinforced fiberglass plastic with good insulation properties. The support blocks and the sliding bearings were mechanically anchored at the bottom of the guard plate, in angle of 120°, respectively. The support blocks were used to support the hot plate, and the sliding bearings were used to move the hot plate to facilitate the installation of the specimens.

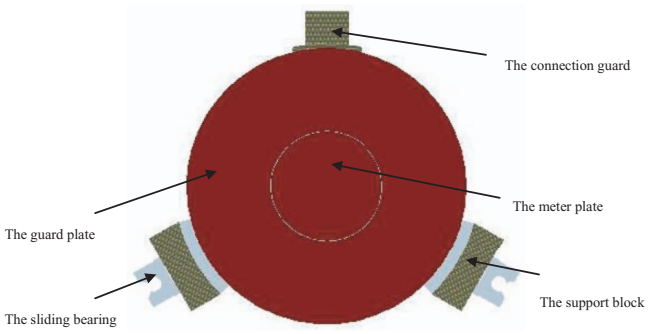

FIG. 4. The structure of the hot plate assembly.

FIG. 5. The multiple heater layouts for the meter plate and guard plate.

The hot plate, of 16 mm in thickness, was made of commercially oxygen-free copper (T2), and consisted of a meter plate with 119.2 mm in diameter and a co-planar concentric guard plate with an inner diameter of 120.8 mm and an outer diameter of 300 mm. The ratio of the outer diameter of the guard plate to the meter plate was of 2.5. The width of the guard gap between the meter plate and the guard plate was of 0.8 mm.

The surfaces of the meter plate, in close contact with the specimens, were quite flat with unevenness less than 0.03 mm. The surfaces of the guard plate in close contact with the specimens were also required flat with unevenness less than 0.05 mm. The working surfaces of the hot plate were coated with a ceramic coating (Cr_2O_3–SiO_2 blend) having an emittance of 0.81.[4]

The surface temperature should be kept constant for the hot plate and the cold plates, which were contacted with the specimens. Therefore, the requirement of the location for the heater was to maintain the temperature profile of the gap equal to the averaged temperature of the meter plate. The circular line-heat sources were used for the meter and guard plates, and were located at prescribed radial location. The heaters were embedded in the zigzag mating grooves cut in the both inner surfaces of the meter and guard plates at a prescribed radius, as shown in Fig. 5.

The layout of the multiple heaters for the meter plate and guard plate were, respectively, ten circular heaters located at corresponding radius, as listed in Table I for n = 5. The heaters of the meter and guard plates were both made of Nickel-chromium.[2]

Where n is the number of line-heat sources, a_1–a_5 are, respectively, the radius of the line-heat sources in the meter plate, c_1–c_5 are, respectively, the radius of the line-heat sources in the guard plate, and b is the diameter of the meter plate.

Temperature homogeneity of the meter plate is a very important factor on the accuracy and precision of the GHP. It is necessary to measure the surface temperature on both sides of the meter plate at the diameter of 30 mm, 60 mm, and 90 mm, respectively. Each of the above diameters matches the test angles of 36°, 72°, 108°, and 144° from horizontal by thin film platinum resistance thermometers. The surface temperature of the meter plate, measured in the experiments, ranges from 25 °C to 70 °C. The maximal temperature difference and standard deviation were shown in Fig. 6.

It was observed that the maximum and standard deviations of the temperature difference on both sides of the surface on the meter plate were less than 0.38 °C and 0.17 °C, respectively. Therefore, it is clear that quantity of heat input to the meter plate was almost equally divided into both specimens.

To minimize the undesired lateral heat flows across the guard gap, the surfaces of the gap were polished to reduce the thermal emissivity. The power input to the guard heater is adjusted in such a way that the temperature difference between the meter plate and guard plate is kept less than 0.1 K and is measured by platinum resistance thermometers (PRTs). The cross-sectional profile of the gap was designed to be a kind of diamond-shaped to maintain a high thermal resistance and to minimize lateral heat flow across the gap. The cross-sectional profile of the gap between the meter and guard plates was shown in Fig. 7.

The heat flow across the gap can be calculated as[2]

$$Q_g \approx \frac{2\pi bm\lambda_g \Delta T_g}{w}\left[\frac{m-2R}{m}+\frac{8w}{\pi m}\times\sum_{n=1,3,5\cdots}^{\infty}\frac{1}{n}\left\{\cos ech\,(n\pi)\cosh\frac{n\pi w}{2R+w}-\coth(n\pi)\cos\frac{2n\pi R}{2R+w}\right\}\right], \quad (5)$$

where Q_g is the heat flow across the gap; m is the plate thickness (16 mm); b is the radius to the center of the gap (60 mm); λ_g is the thermal conductivity of 3 μm glass fiber insulation in the gap (0.035 W/m K); ΔT_g is the temperature difference across the gap (less than 0.1 K); w is the width of the gap (0.8 mm); and $2R$ is the vertical distance of the meter plate subtended by the angle of the diamond-shaped cross section (6.3 mm).

B. Cold plate assemblies

The cold plate assemblies were designed to provide the isothermal surfaces in close contact with the specimens and to remove the heat generated by the hot plate. The structure of the cold plate assembly was shown in Fig. 8, which consisted of: (1) The liquid nitrogen container; (2) the support blocks;

TABLE I. Radial locations for line-heat sources in the meter and guard plates.

	a_1/b	a_2/b	a_3/b	a_4/b	a_5/b	c_1/b	c_2/b	c_3/b	c_4/b	c_5/b
$n = 5$	0.1531	0.3408	0.5296	0.7183	0.9074	1.1544	1.4531	1.7527	2.0522	2.3521
Radius (mm)	9.186	20.448	31.776	43.098	54.444	69.264	87.186	105.162	123.132	141.126

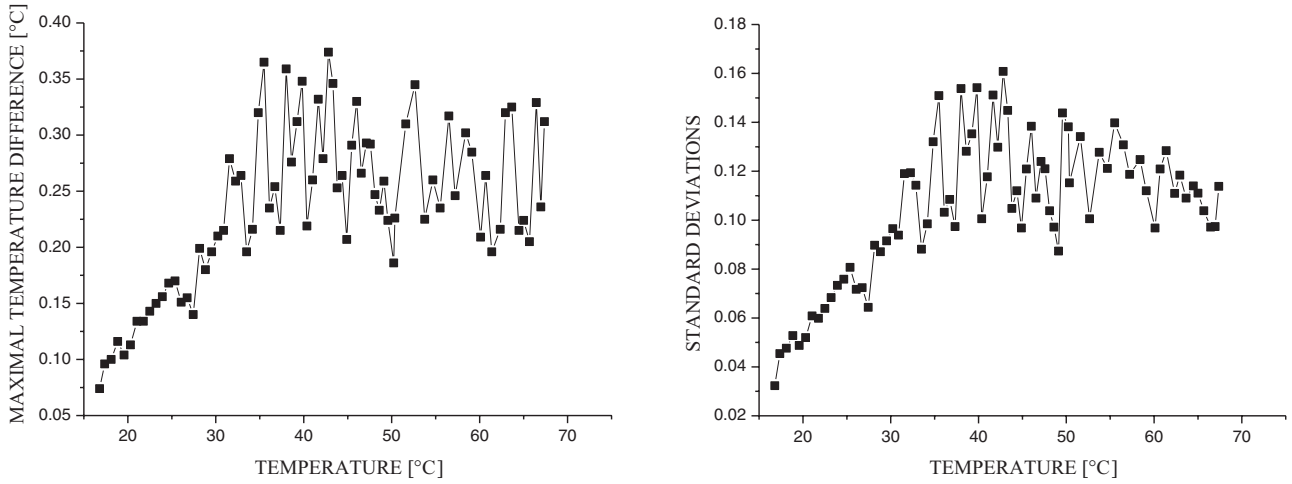

FIG. 6. The maximum and standard deviations of the temperature difference on the both sides of the meter plate.

(3) the sliding bearings; (4) the inlet of the liquid nitrogen; and (5) the outlet of the gaseous nitrogen.

The liquid nitrogen containers were fabricated from the austenitic stainless steel. The surfaces of the liquid nitrogen containers were in close contact with the specimens with unevenness less than 0.05 mm. The working surfaces of the liquid nitrogen containers were coated with a ceramic coating (Cr_2O_3–SiO_2 blend) having an emittance of 0.81.[4]

In the experiments, the liquid nitrogen was transported into the liquid nitrogen container by the liquid nitrogen transport pipes. As the liquid nitrogen absorbed the heat transferred from the specimens in contact, the evaporated nitrogen gas was discharged from the vacuum chamber by the outlet of the gaseous nitrogen.

The support blocks and the sliding bearings were fixed at the bottom of the liquid nitrogen containers, and their located positions were the same as that of the hot plate.

C. Vacuum chamber

The vacuum vessel was constructed with the austenitic stainless steel and it consisted of a cylinder 800 mm in diameter and 600 mm in length, an ellipsoidal head, and a vessel flange. The vacuum vessel was mechanically welded onto a support frame, and was bolted to an operating platform. A JTK-300 vacuum diffusion pump unit was connected at the centerline of the ellipsoidal head by a stainless steel sylphon bellows. The leakage rate of the vacuum vessel was $\sim 1 \times 10^{-10}$ standard Pa m^3/s. The vacuum of the vacuum chamber was measured by an ionization vacuum gauge.

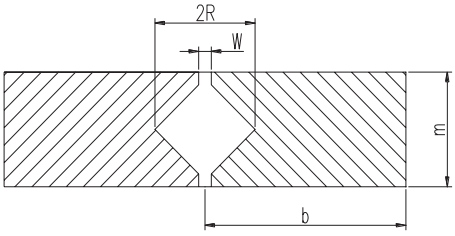

FIG. 7. The cross-sectional profile of the gap between the meter and guard plates.

D. Other assemblies

The clamping assemblies were used to guarantee good thermal contact between the hot, cold surface assemblies and the specimens, and to maintain equal spacing between the hot and cold assemblies as well.

The clamping assemblies consisted of the insulation blocks, the compression springs, and the clamping bolts. The reinforced fiberglass plastics were employed as the insulation blocks to reduce the heat transfer through the clamping assemblies.

The suspension assemblies were welded onto the top of the vacuum vessel. The whole test component was suspended from the suspension assemblies to minimize the undesired evaporation of liquid nitrogen.

IV. MEASUREMENT PROCEDURES

The thermal conductivity of the insulations depends on the precise monitor of the input power of the meter plate, the accurate measurements of the temperatures, the meter area,

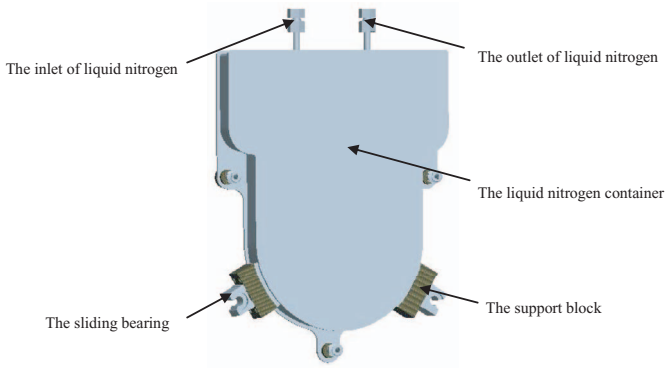

FIG. 8. The structure of the cold plate assembly.

the thickness of the specimens, and a well-controlled heat flow across the guard plate.

A. The power to the meter plate

The heat flow through each specimen is equal to the half of the input power generated by the heater inserted in the meter plate. The input power consumption of the meter plate is depended on the diameter, the thickness and thermal conductivity of the specimens under test. A digital direct current power supply provides the adjustable current and voltage to the heater in the meter plate. The input power supplied to the meter plate is determined by measuring the voltage drop across the heater and the corresponding current. The input power of the meter plate, Q are then calculated by voltage drop (V_m) and current (I_m) as follows:

$$Q = V_m \times I_m. \tag{6}$$

B. The temperature

In order to obtain accurate thermal conductivity of insulations, it is necessary to measure accurately the average temperature difference on both sides of specimens. In addition, the temperature variance of the meter plate should be kept smaller by adjusting the input power of the guard plate to reduce the heat gains or losses to the meter plate.

The temperature sensors adequately sample the meter area if there were significant temperature variations. The temperatures of the meter plate were measured by three thin film PRTs. The PRTs were uniformly located at the periphery of the meter plate at azimuthal angles of 69°, 180°, and 291°. The temperatures of the guard plate were measured by four thin film PRTs, which were installed around the inner edge of the guard plate at 45°, 135°, 225°, and 315°. Figure 9 showed the locations of the PRTs in the meter plate and guard plate.

Similarly, three PRTs were used on the surface of the cold plate assemblies, and they were placed at the same angles and positions as the meter plate.

C. The meter area and thickness of the specimens

The meter area is defined as the summary of the surface areas of the meter plate and one-half the guard gap. After the meter plate and guard plate were manufactured and assembled, the meter area was then fixed.

The thickness of the specimens was measured before and after the thermal conductivity of insulation was measured, in order to check if there was any change. Any warping or bowing of the specimen before or during measurement of the thermal properties, would add the uncertainty in the measurements of the thickness.[15]

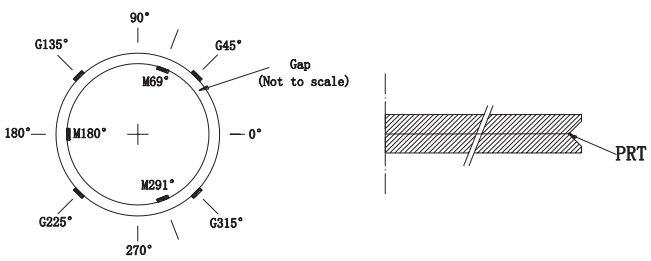

FIG. 9. Locations of the PRTs in meter and guard plates. (a) Angular locations of the PRTs in guard gap. (b) Cross-section view of the PRTs in the gap.

V. VALIDATION OF PERFORMANCE

In this section, the data comparisons of the thermal conductivity of samples were conducted for the designed GHP operating down to liquid nitrogen temperature. The teflon plates with 4 mm ± 0.1 mm in thickness and 300 mm in diameter were used here as calibration samples. The measuring system was first evacuated to a sufficiently high vacuum ($<10^{-2}$ Pa) using a diffusion pumping station. The input dc power to the meter and the guarded plates was adjusted until the temperature differences were less than 0.1 K. When these conditions were in a stable state, the temperature and power were recorded at interval of 30 s. The comparison of thermal conductivity of experimental results and that of published results of teflon plates in the temperature range from 77 K to 180 K, as shown in Fig. 10.[17,18] It was observed that the maximum deviations of the thermal conductivities were about 6%. The results of repetitive experiments showed that the variations were within ±2%.

VI. PRECISION AND BIAS

The precision and bias of the test data have a direct effect on the result. The uncertainties of the thermal conductivity are associated with the emissivity, the expansivity, the hygroscopicity, the density, the area and thickness of thermal insulations. Therefore, it is necessary to assess the precision and bias of the test data.

The uncertainty assessment of the apparatus is based on the consideration of the random and systematic errors. The

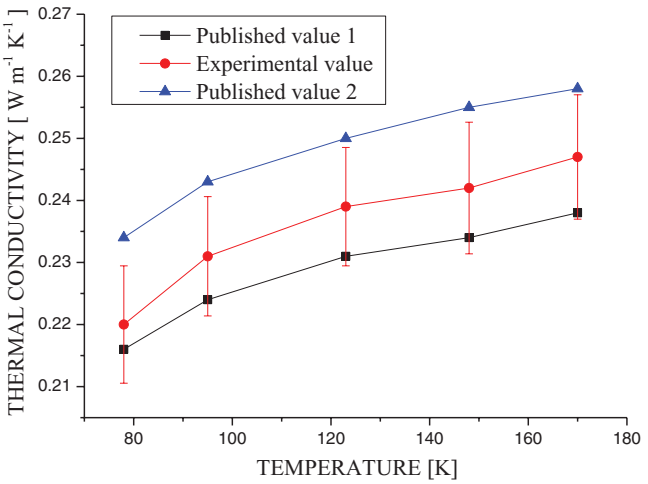

FIG. 10. Comparison of experimental and published values of thermal conductivity.

errors in experimental measurements come from the uncertainties in terms of the heat flow δQ, the temperature difference $\delta\Delta T$, the meter area δA, and the specimen thickness δL.

The combined standard uncertainty of a measurement result, $u_c(y)$, is expressed as the positive square root of the combined variance $u_c^2(y)$

$$u_c(y) = \sqrt{\sum_{i=1}^{n} c_i^2 u^2(x_i)}, \tag{7}$$

where the sensitivity coefficients (c_i) are equal to the partial derivative of an input quantity $(\partial f/\partial X_i)$ evaluated for the input quantity equal to an input estimate $(X_i = x_i)$; $u(x_i)$ is the standard uncertainty associated with the input estimate x_i.

The combined standard uncertainty $u_c^2(y)$ is defined by Eq. (7). In the mathematical model, Eq. (1), all input quantities are assumed uncorrelated. Thus, the combined standard uncertainty in the thermal conductivity can be calculated from the following error propagation formula:

$$u_c(\bar{\lambda}) = \sqrt{c_Q^2 u_c^2(\bar{Q}) + c_L^2 u_c^2(\bar{L}) + c_A^2 u_c^2(\bar{A}) + c_{\Delta T}^2 u_c^2(\Delta\bar{T})}, \tag{8}$$

where

$$c_Q = \partial\bar{\lambda}/\partial\bar{Q} = \frac{L}{A(\Delta T)}, \tag{9}$$

$$c_L = \partial\bar{\lambda}/\partial\bar{L} = \frac{Q}{A(\Delta T)}, \tag{10}$$

$$c_A = \partial\bar{\lambda}/\partial\bar{A} = \frac{-QL}{A^2(\Delta T)}, \tag{11}$$

$$c_{\Delta T} = \partial\bar{\lambda}/\partial\Delta\bar{T} = \frac{-QL}{A(\Delta T)^2}. \tag{12}$$

The selected PRTs have been calibrated with the temperature range from 54.285 K to 351.04 K. The maximum deviation of temperature is 4.7 mK. Therefore, the uncertainty $u(\Delta\bar{T})$ of the temperature difference is

$$u_c(\Delta\bar{T}) = \sqrt{(4.7\times10^{-3})^2 + (4.7\times10^{-3})^2} = 6.65\times10^{-3}\,\mathrm{K}, \tag{13}$$

and the variance

$$u_c^2(\Delta\bar{T}) = 4.42\times10^{-5}\,\mathrm{K}^2. \tag{14}$$

The input power of the meter plate is determined by the voltage drop and the current of the heater through the direct current power supply. The product specifies a resolution of 10 μV and the maximum permissible error of 10×10^{-6} the voltage reading 2×10^{-6} V for the voltage ranging from 0 to 36 V. For the measured maximum value of $U = 20$ V, and the measured value $U_R = 0.5$ V, the uncertainty and variance in absolute terms are as follows:

$$u_c(\bar{U}) = [(10\times10^{-6}\times20) + (2\times10^{-6}\times36)]/\sqrt{3} = 1.57\times10^{-4}\,\mathrm{V}, \tag{15}$$

$$u_c^2(\bar{U}) = 2.47\times10^{-8}\,\mathrm{V}^2, \tag{16}$$

$$u_c(\bar{U}_R) = [(10\times10^{-6}\times0.5) + (2\times10^{-6}\times36)]/\sqrt{3} = 7.04\times10^{-5}\mathrm{V}, \tag{17}$$

$$u_c^2(\bar{U}_R) = 4.96\times10^{-9}\,\mathrm{V}^2. \tag{18}$$

The certificated standard resistor $R = 1\ \Omega$, specifies a resolution of $5\times10^{-6}\ \Omega$, so that the uncertainty and the variance are given by

$$u_c(\bar{R}) = 5\times10^{-6}/2.58 = 1.94\times10^{-6}\Omega, \tag{19}$$

$$u_c^2(\bar{R}) = 3.76\times10^{-12}\,\Omega^2. \tag{20}$$

As a result, the combined standard uncertainty in the input power of the meter plate can be obtained from the following error propagation formula:

$$u_c^2(\bar{Q}) = \left(\frac{U_R}{R}\right)^2 u_c^2(\bar{U}) + \left(\frac{U}{R}\right)^2 u_c^2\left(\bar{U}_R\right) + \left(\frac{UU_R}{R^2}\right)^2 u_c^2\left(\bar{R}\right) = 2.03\times10^{-6}. \tag{21}$$

The uncertainty of the meter area depends on the precision of the processing technology, as well as the accuracy of the assembly process. The caliper specifies a resolution of 0.01 mm. The uncertainty and variance in absolute terms are as follows:

$$u_c(\bar{A}) = 3.1415\sqrt{\left(0.1\times\frac{1\times10^{-5}}{\sqrt{3}}\right)^2 + \left(0.1\times\frac{1\times10^{-5}}{\sqrt{3}}\right)^2} = 1.28\times10^{-5}\,\mathrm{m}^2, \tag{22}$$

$$u_c^2(\bar{A}) = 1.65\times10^{-10}\,\mathrm{m}^4. \tag{23}$$

The uncertainty and variance of the thickness in absolute terms are as follows:

$$u_c(\bar{L}) = 1\times10^{-5}/\sqrt{3} = 5.80\times10^{-6}\,\mathrm{m}, \tag{24}$$

$$u_c^2(\bar{L}) = 3.33\times10^{-11}\,\mathrm{m}^2. \tag{25}$$

The combined standard uncertainty in the thermal conductivity was assigned to the measurement result on the above-mentioned calibration samples operated down to liquid nitrogen temperature (−196 °C). The combined standard uncertainty in absolute terms is as follows:

$$u_c(\bar{\lambda}) = \sqrt{c_Q^2 u_c^2(\bar{Q}) + c_L^2 u_c^2(\bar{L}) + c_A^2 u_c^2(\bar{A}) + c_{\Delta T}^2 u_c^2(\Delta\bar{T})} = 3.24\times10^{-4}\ \mathrm{W/(m\,K)}. \tag{26}$$

An expanded uncertainty of measurement $U_c(\bar{\lambda}) = 2u_c(\bar{\lambda})$ was stated. The coverage probability for the coverage factor 2

is 95%. The uncertainty of measurement of the sample is

$$U_c(\bar{\lambda}) = 2 \times 3.24 \times 10^{-4} = 6.48 \times 10^{-4}\ \mathrm{W/(m\ K)}. \quad (27)$$

The measurement result for the teflon plates is $\lambda = 0.22 \pm 6.48 \times 10^{-4}$ W/(m K).

VII. CONCLUSION

A double-sided GHP for the thermal conductivities of insulation specimens operated down to liquid nitrogen temperature (−196 °C) was designed and constructed. The structural arrangement and the method of the line-heat sources were different from that of the traditional GHP. The analysis of the measurement uncertainty conducted on teflon plates showed that the results were in good agreement with a standard deviation less than ±6%. Therefore, the new designed GHP can accurately measure the thermal conductivity of insulations operated down to liquid nitrogen temperature.

ACKNOWLEDGMENTS

This work is supported by National Natural Science Foundation of China (NNSFC) (Grant No. 51006069).

[1] D. R. Flynn, R. R. Zarr, W. Healy, and M. H. Hahn, Insul. Mater. Test. Appl. **4**, 98 (2002).
[2] ASTM Practice C 1043, *Annual Book of ASTM Standards*, Vol. 04.06, 2010.
[3] W. Hemminger and R. Jugel, Int. J. Thermophys. **6**, 483 (1985).
[4] R. R. Zarr, D. R. Flynn, J. W. Hettenhouser, N. J. Brandenburg, and W. M. Healy, ITCC 28/ITES 16, St. Andrews, New Brunswick, Canada, 2005.
[5] B. J. Filla, Rev. Sci. Instrum. **68**, 2822 (1997).
[6] D. R. Flynn, W. M. Healy, and R. R. Zarr, Thermal Conductivity 28/Thermal Expansion 16 Joint Conferences, New Brunswick, Canada, 2005.
[7] M. H. Hahn, H. E. Robinson, and D. R. Flynn, Heat Transm. Meas. Therm. Insul. 167–192 (1974).
[8] J. Xaman, L. Lira, and J. Arce, Appl. Therm. Eng. **29**, 617 (2009).
[9] C. J. Dey, T. M. Simko, R. E. Collins, and Q. C. Zhang, Rev. Sci. Instrum. **69**, 2939 (1998).
[10] W. Woodside, Rev. Sci. Instrum. **28**, 1033 (1957).
[11] B. V. Holcombe, Rev. Sci. Instrum. **55**, 1464 (1984).
[12] E. V. Somers and J. A. Cyphers, Rev. Sci. Instrum. **22**, 583 (1951).
[13] Q. T. Pham and C. G. Smith, Rev. Sci. Instrum. **57**, 99 (1986).
[14] Q. T. Pham, Rev. Sci. Instrum. **58**, 660 (1987).
[15] ASTM Standard Test Method C 177-04, *Annual Book of ASTM Standards*, Vol. 04.06, 2004.
[16] T. K. Lim, B. P. Axcell, and M. A. Cotton, Appl. Therm. Eng. **27**, 1352 (2007).
[17] S. Kanagaraj and S. Pattanayak, Cryogenics **43**, 451 (2003).
[18] K. D. Timmerhaus and T. M. Flynn, *Cryogenics Process Engineering* (Plenum, New York, 1989).